arXiv:2101.05600v3 [eess.AS] 11 Sep 2021

FAST OFFLINE TRANSFORMER-BASED END-TO-END AUTOMATIC SPEECH RECOGNITION FOR REAL-WORLD APPLICATIONS

PREPRINT

Yoo Rhee Oh, Kiyoung Park [*], Jeon Gue Park
Artificial Intelligence Research Laboratory
Electronics and Telecommunications Research Institute (ETRI)
Daejeon, Republic of Korea

November 25, 2021

ABSTRACT

With the recent advances in technology, automatic speech recognition (ASR) has been widely used in real-world applications. The efficiency of converting large amounts of speech into text accurately with limited resources has become more important than ever. This paper proposes a method to rapidly recognize a large speech database via a Transformer-based end-to-end model. Transformers have improved the state-of-the-art performance in many fields. However, they are not easy to use for long sequences. In this paper, various techniques to speed up the recognition of real-world speeches are proposed and tested, including decoding via multiple-utterance batched beam search, detecting end-of-speech based on a connectionist temporal classification (CTC), restricting the CTC prefix score, and splitting long speeches into short segments. Experiments are conducted with the Librispeech English and the real-world Korean ASR tasks to verify the proposed methods. From the experiments, the proposed system can convert 8 hours of speeches spoken at real-world meetings into text in less than 3 minutes with a 10.73% character error rate, which is 27.1% relatively lower than that of conventional systems.

Keywords Speech recognition, Transformer, end-to-end, connectionist temporal classification

1 Introduction

Owing to the rapid advances in automatic speech recognition (ASR) research et al [2019a], Roger et al. [2020], et al [2020a], Chung et al. [2019], these technologies have been widely adopted in many practical applications, such as automatic response systems, automatic subtitle generation, and meeting transcription. Deep neural network (DNN) incorporated with the traditional hidden Markov Model (HMM) has worked powerfully and raised speech recognition accuracy to the commercial level.

A recent breakthrough in deep learning from natural language processing solved sequence generation problem in a novel way Sutskever et al. [2014], Bahdanau et al. [2015]. Further, a Transformer model in which sequences are processed more thoroughly with self-attention achieves state-of-the-art performances in many tasks.

In ASR, where the speech recognition problem is formulated as generation of the most probable sequence of words given a spoken utterance as an input sequence, a Transformer-based end-to-end speech recognition technique has achieved state-of-the-art performance and a major breakthrough since deep learning technology was used with HMM et al [2017a], Dong et al. [2018].

However, it is well-known that the Transformer is not sufficient at processing long sequences with regard to performance and computation speed, and speech signals are usually represented by much longer sequences than the written sentence. There have been many research studies attempting to overcome this drawback, including Moritz et al. [2019, 2020], Hwang and Lee [2020].

[*]*Corresponding author: Kiyoung Park, pkyoung@etri.re.kr

There is an abundance of speeches already recorded and published that needs to be transcribed, and more data are being generated every day Parthasarathi and Strom [2019]. Hence, it is important to recognize large speech databases very quickly at the lowest cost. In this work, we present efficient methods to utilize the Transformer in continuously spoken long speech recognition.

1.1 Literature review

In 2017, a deep learning model, Transformer, was introduced for machine translation tasks et al [2017a]. Transformer has been adopted in many natural language processing tasks and produced significant performance improvements. In 2018, Transformer was adopted for speech recognition tasks with significant improvements when compared to recurrent neural network (RNN)-based speech recognition Dong et al. [2018], Zhou et al. [2018], et al [2018a]. Accordingly, there have been many studies on Transformer-based end-to-end speech recognition, which achieved state-of-art speech recognizers et al [2019b, 2020b,c]. Moreover, et al [2019c] successfully integrated connectionist temporal classification (CTC) into Transformer-based end-to-end speech recognition for faster training, and subsequently improved the speech recognition performance. Recently, a joint CTC/Transformer approach was used in various research studies et al [2019b], Moritz et al. [2020], et al [2020d,e,f,g], Parcollet et al. [2020], et al [2020h,i,j,k,l,m,n,o,p]. Therefore, this paper focuses on CTC/Transformer-based end-to-end speech recognition.

To increase the throughput of RNN-based speech recognizers, et al [2016, 2020q], Oh et al. [2020] utilized several batch processing approaches. In particular, et al [2020q], Oh et al. [2020] aimed to accelerate GPU parallelization. Seki et al. [2018], et al [2019d] proposed a multiple-utterance multiple-hypothesis vectorized beam search in CTC-attention-based end-to-end speech recognition using a VGG-RNN-based encoder-decoder and showed the decoding throughput increase using a GPU. Motivated by Seki et al. [2018], et al [2019d], we aim to successfully adopt the vectorized beam search in CTC/Transformer-based end-to-end speech recognition for faster and more efficient decoding of a large speech database.

The CTC prefix decoding used in CTC/Transformer end-to-end speech recognition requires computation over an entire input sequence for each iteration et al [2006] and is not parallel processing but sequential processing, which hinders the GPU parallelization. Since this is a bottleneck in fast processing, several time-restricted CTC prefix decoding methods et al [2019d, 2020r] have been proposed. et al [2019d] proposed a windowing method using attention weights of a VGG-RNN decoder network with the assumption that the time alignment of the CTC prefix decoding is similar to that of the attention decoding. et al [2020r] proposed truncated CTC prefix decoding using the previous and current CTC probabilities of a blank symbol at each iteration. For fast decoding, we propose time-restricted CTC prefix decoding via a different method.

Voice activity detection (VAD) is one solution for decoding long utterances robustly with low resources in an end-to-end speech recognizer et al [2020s]. et al [2020s] proposed a CTC-based VAD integrated into an end-to-end speech recognizer and compared this to an energy-based VAD method and time-delay neural network (TDNN)-based VAD. This paper proposes a DNN-based VAD with a different method for the vectorized beam search in CTC/Transformer end-to-end speech recognition.

1.2 Proposed Method and Its Contribution

In this paper, we propose a method to recognize a large speech database very quickly and cost-effectively for CTC/ Transformer-based end-to-end speech recognition. To this end, we adopt the multiple-utterance multiple-hypothesis vectorized beam search decoding of et al [2019d, 2020r] in Transformer-based speech recognition. We observed that the baseline end-of-speech detection method fails if an abnormal utterance is encountered since the method is based on the absolute value of CTC probability. Thus, we propose an end-of-speech detection method using CTC-based time information. To reduce the deterioration of GPU parallelization, CTC prefix decoding is moved from the GPU to the CPU. To unburden the CPU processing load, we propose a time-restricted CTC prefix decoding method using the previous CTC probabilities of the target symbol and its blank symbol for each iteration because it is difficult to determine the time information from a Transformer decoder, unlike et al [2019d, 2020r]. Another issue is the limited GPU memory size since batchfied utterances are padded with the maximum utterance length before the vectorized beam search Seki et al. [2018], et al [2019d]. Therefore, we propose a method to segment long speeches into smaller pieces for batch decoding, and create a batch having speech segments of similar lengths.

The contributions of this paper are summarized as follows:

Multiple-utterance multiple-hypothesis batched beam search for Transformer As a prior work, multiple-utterance multiple-hypothesis batched decoding was utilized for a joint CTC/Attention-based VGG-RNN. Motivated by this prior work, we extend the multiple-utterance batched decoding for Transformer-based speech recognition.

Time-restricted CTC prefix scoring for Transformer Influenced by time-restricted CTC prefix scoring for a VGG-RNN-based model, we present time-restricted CTC prefix scoring using CTC-based time information instead of attention weights.

Improvement in end-of-speech detection We propose an improved end-of-speech detection based on estimated time information. That is, conventional end-of-speech detection works well in matched conditions with speeches in training corpus, but if an abnormal speech is encountered, then the method could fail to detect end-of-speech. Thus, the decoding efficiency is degraded. To solve this problem, we improve conventional end-of-speech detection.

Utterance segmentation for efficient decoding with the Transformer In order to efficiently manipulate GPU-based batched beam search decoding for the Transformer, it is important to split utterances to be decoded. First, we adopted a DNN-VAD based segmentation to split at pauses. Using this method, the decoding speed can be significantly accelerated with little accuracy degradation. Then, it is shown that hard segmentation can be also used as a splitting method with minor accuracy degradation. It is also analyzed that sorting and making batches of utterances of similar lengths helps to speed up the decoding. By integrating these techniques, we can deploy highly efficient end-to-end speech recognizers for real-world applications.

The remainder of this paper is organized as follows. Section 2 reviews a CTC/Transformer-based speech recognition in brief. In Section 3, the methods we utilized to speed up the recognition for large speech corpus are presented. Next, in Section 4, the performance of the proposed speech recognition is evaluated with a public dataset and a real-world meeting corpus spoken by multiple speakers. Finally, we conclude the paper with our findings in Section 5.

2 CTC/Transformer-based speech recognition

The authors of et al [2017a] propose a sequence-to-sequence attention-based encoder-decoder network, Transformer, for a neural machine translation task. With an outstanding performance, Transformer is successfully adopted in speech recognition Dong et al. [2018], et al [2018a, 2019b] and this work also adopts the Transformer network of et al [2019b]. As shown in Fig. 1, the encoder network consists of sub-sampling, input embedding, position encoding, N_e encoder blocks, and normalization layers. The decoder network consists of output embedding, positional encoding, N_d decoder blocks, normalization, linear, and softmax layers. A linear layer and a softmax are also used for a CTC decoder, which is shown in orange-line in the figure. Each encoder block consists of multi-head attention and feed-forward layers. Each decoder block consists of masked multi-head attention, multi-head attention, and feed-forward. Layer normalization is applied before each multi-head attention and feed-forward and residual addition is applied after each of them. The following subsections briefly explain a joint CTC/Transformer score and a beam search decoding for speech recognition inference.

2.1 Joint CTC/Transformer score

In et al [2019c,d], a joint CTC/attention decoding is performed to maximize the logarithmic linear combination of the sequence probabilities that are obtained by the Transformer and CTC decoders. For the l-length sequence, $\mathbf{y}^{1:l}$, of a speech representation, $\mathbf{h}$, this work calculates a joint CTC/Transformer score et al [2019c] as follows,

$$P^{\text{joint}}(\mathbf{y}^{1:l}|\mathbf{h}) = \lambda P^{\text{CTC}}(\mathbf{y}^{1:l}|\mathbf{h}) + (1-\lambda)\, P^{\text{Att}}(\mathbf{y}^{1:l}|\mathbf{h}), \tag{1}$$

where $P^{\text{CTC}}(\mathbf{y}^{1:l}|\mathbf{h})$ and $P^{\text{Att}}(\mathbf{y}^{1:l}|\mathbf{h})$ are the CTC prefix probability and the attention probability respectively. And λ is the CTC weight.

The attention probability, $P^{\text{Att}}(\mathbf{y}^{1:l}|\mathbf{h})$, is calculated as,

$$P^{\text{Att}}(\mathbf{y}^{1:l}|\mathbf{h}) = P^{\text{Att}}(\mathbf{y}^{1:l-1}|\mathbf{h}) + p^{a}(\mathbf{y}^{l}|\mathbf{y}^{1:l-1}, \mathbf{h}) \tag{2}$$

where $p^{a}(\mathbf{y}^{l}|\mathbf{y}^{1:l-1}, \mathbf{h})$ is the attention output probability at time l given $\mathbf{y}^{1:l-1}$ and $\mathbf{h}$, as shown in Fig. 1.

Next, CTC et al [2006] maps a frame-wise speech feature vector to a token-wise output sequence in a monotonic manner. Let $\mathbf{h}$ be a frame-wise T-length speech representation and $\mathbf{y}_{1:L}$ be a token-wise L-length output sequence, $\mathbf{y}_{1:L} = \{y_l \in C | l = 1, \cdots, L\}$, with a token set C. The CTC introduces a frame-wise T-length output sequence, $Z = \left\{ z_t \in \hat{C} | t = 0, \cdots, T \right\}$, with an extended token set $\hat{C} = \{C \cup \text{blank}\}$. z_t can be defined as,

$$\text{blank}, \qquad \text{if } t = 0 \tag{3}$$

$$y^{l-1} \text{ or } y^{l} \text{ or blank}, \qquad \text{if } z_{t-1} = y^{l-1} \text{ and } y^{l-1} \neq y^{l} \tag{4}$$

$$y^{l-1} \text{ or blank}, \qquad \text{if } z_{t-1} = y^{l-1} \text{ and } y^{l-1} = y^{l} \tag{5}$$

$$y^{l} \text{ or blank}, \qquad \text{if } z_{t-1} = \text{blank and } z^{nb}_{t-1} = y^{l-1} \tag{6}$$

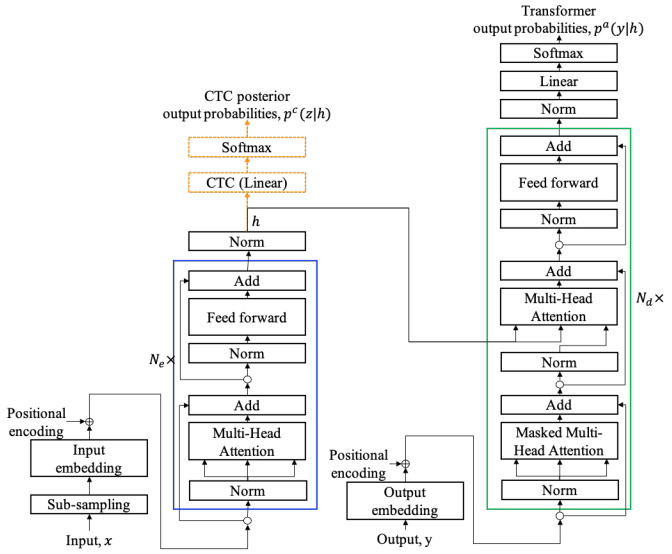


Figure 1: Overall structure of the CTC/Transformer-based speech recognizer that is used in this work et al [2019b]. Encoder blocks and decoder blocks are depicted in blue-line and in green-line, respectively. A CTC decoder is shown in orange-line.

where the first and last non-blank tokens are y^1 and y^L. z_t^{nb} is the previous non-blank token up to t. The best output sequence of Z is obtained by finding a sequence that maximizes a CTC prefix probability Hori et al. [2017], et al [2019d, 2020r]. The CTC prefix probability accumulates the probabilities of all possible sequences having a prefix sequence. That is, for an l-length hypothesis $\mathbf{y}^{1:l}$ of a speech representation $\mathbf{h}$, the CTC prefix probability, $P^{\mathrm{CTC}}(\mathbf{y}^{1:l}|\mathbf{h})$, is calculated as,

$$\sum_{l\leq t\leq T} \phi_{t-1}(\mathbf{y}^{1:l-1}|\mathbf{h})p^c(z_t = \mathbf{y}^l|\mathbf{y}^{1:l-1}, \mathbf{h}), \tag{7}$$

where $\phi_{t-1}(\mathbf{y}^{1:l-1})$ is the CTC forward probability up to time $t-1$ for $\mathbf{y}^{1:l-1}$. $p(z_t|\mathbf{y}^{1:l-1}, \mathbf{h})$ is the CTC posterior probability at time t given $\mathbf{y}^{1:l-1}$ and $\mathbf{h}$, as shown in Fig. 1.

2.2 Beam search decoding

This work uses a beam search decoding Meister et al. [2020] to find the output sequence for an input utterance. The beam search is a beam-pruned breadth-first search, as summarized in Algorithm 1. Let $\mathbf{x}$ be a speech feature. Using a Transformer encoder, $\mathbf{x}$ is converted into the intermediate representation $\mathbf{h}$ where $|\mathbf{h}|$ is the length of $\mathbf{h}$. Then, $\mathbf{h}$ is converted into the text sequence $\mathbf{y}$ by performing the B-width beam search where Eq. 1 is used as the scoring function to evaluate the reliability of a hypothesis (line 3 of Algorithm 1).

At the l-th step of the beam search, the l-length hypothesis scores, $\mathbf{P}_{[|C|]}$, are calculated using $\mathbf{h}$, $\mathbf{Y}^{l-1}$, and C (line 7 of Algorithm 1)). It is noted that the notation $A_{[B]}$ means that a matrix A has the shape of B. $\mathbf{I}_{[B]}$ is obtained by selecting the indices of the B highest scores of $\mathbf{P}_{[|C|]}$ (line 10 of Algorithm 1). Then, the l-length hypothesis set, $\mathbf{Y}^l_{[B]}$, is obtained by selecting the l-length reliable hypotheses using $\mathbf{Y}^{l-1}$, C, and $\mathbf{I}_{[B]}$ (line 11 of Algorithm 1). It is noted that $a \circ B$ indicates that a is concatenated with each item of B. Next, $\hat{\mathbf{Y}}$ is updated if <*eos*>-ended hypothesis is confident (lines 12–15 of Algorithm 1).

The beam search is terminated if the decoding step l is greater than $|\mathbf{h}|$ (line 4 of Algorithm 1) or if end-of-speech is detected (lines 17–19 of Algorithm 1). Finally, the output sequence is obtained with the most probable hypothesis in $\hat{\mathbf{Y}}$ (line 21 of Algorithm 1).

Algorithm 1 B-width beam search decoding

Input: input feature representation **h**, beam width B
Output: output sequence y
1: $\mathbf{Y}^0 \leftarrow \{$<*eos*>$\}$
2: $\hat{\mathbf{Y}} \leftarrow \varnothing$
3: score_fn$(\cdot) \leftarrow P^{\text{joint}}(\cdot|\mathbf{h})$
4: **for** $l \in \{1, \cdots, |\mathbf{h}|\}$ **do**
5: $\quad \mathbf{Y}^l \leftarrow \varnothing$
6: $\quad$ **for** $y \in \mathbf{Y}^{l-1}$ **do**
7: $\quad\quad \mathbf{P}_{[|C|]} \leftarrow$ score_fn(y)
8: $\quad\quad \hat{\mathrm{P}} \leftarrow \mathbf{P}_{[|C|]}$ (<*eos*>)
9: $\quad\quad \mathbf{P}_{[|C|]}$ (<*eos*>) $\leftarrow$ log0
10: $\quad\quad \mathbf{I}_{[B]} \leftarrow$ topB($\mathbf{P}_{[|C|]}$)
11: $\quad\quad \mathbf{Y}^l_{[B]} \leftarrow$ gatherB($y \circ C$, $\mathbf{I}_{[B]}$)
12: $\quad\quad$ best_score = $max\mathbf{P}_{[|C|]}$
13: $\quad\quad$ **if** $\hat{\mathrm{P}} >$ best_score **then**
14: $\quad\quad\quad \hat{\mathbf{Y}}$.add($\left(y \circ$ <*eos*>$, \hat{\mathrm{P}}\right)$)
15: $\quad\quad$ **end if**
16: $\quad$ **end for**
17: $\quad$ **if** ENDDETECT($\hat{\mathbf{Y}}$, l) == true **then**
18: $\quad\quad$ **break**
19: $\quad$ **end if**
20: **end for**
21: **return** $\text{argmax}_{(y,p)\in\hat{\mathbf{Y}}}\, p$

3 Fast and efficient Transformer-based speech recognition

3.1 Fast decoding based on batched beam search

GPU parallelization can be accelerated by batch processing et al [2019d], Oh et al. [2020], Seki et al. [2018], et al [2016, 2020q]. As in et al [2019d], Seki et al. [2018], we adopt a multiple-utterance multiple-hypothesis batched beam search for a Transformer-based end-to-end speech recognizer to efficiently parallelize speech recognition for multiple utterances. The batched beam search is briefly described in the following, and the detailed explanation is in et al [2019d].

Let $\mathbf{X} = \{\mathbf{x}_1, \cdots, \mathbf{x}_U\}$ be the speech features that are obtained from U utterances. $\mathbf{X}$ is batched as $\mathbb{X} = \{\mathbf{x}_1, \cdots, \mathbf{x}_U\}$ where $\mathbf{x}_i$ is length-extended from x_i. The length is $\max_{\mathbf{x}_i\in\mathbf{X}}|\mathbf{x}_i|$ and the extended values are padded with zeroes. Using a Transformer encoder, $\mathbb{X}$ is converted into the intermediate representations $\mathbb{H} = \{\mathbf{h}_1, \cdots, \mathbf{h}_U\}$, where each of them can be converted in parallel. Then, $\mathbb{H}$ is decoded into the text sequence set $\mathbb{Y} = \{\mathbf{y}_1, \cdots, \mathbf{y}_U\}$ by performing a B-width batched beam search. For the scoring function, Eq. 1 is used to evaluate each hypothesis of $\mathbb{H}$ in parallel (line 3 of Algorithm 2).

At the l-th step of the batched beam search, the score set, $\mathbb{P}_{[U\times B,|C|]}$, of B l-length hypotheses of U speech features is calculated using $\mathbb{H}$, $\mathbb{Y}^{l-1}$, and C, where each score can be calculated in parallel (line 6 of Algorithm 2). $\mathbb{I}_{[U,B]}$ is obtained by selecting the indices of the B highest scores of the U speech feature using $\mathbb{P}_{[U\times B,|C|]}$ (line 9 of Algorithm 2). Then, the l-length hypothesis set, $\mathbb{Y}^l_{[U\times B]}$, is obtained by selecting the B l-length reliable hypotheses for each speech feature using $\mathbb{Y}^{l-1}$, C, and $\mathbb{I}_{[U\times B,B]}$ (line 10 of Algorithm 2). Next, confident <*eos*>-ended hypotheses for each utterance are added into $\hat{\mathbb{Y}}\,(i)$ (lines 11–18 of Algorithm 2).

The beam search is terminated if the decoding step l is greater than $\text{len}_h = \max_{h_i\in\mathbb{H}}|h_i|$ (line 4 of Algorithm 2) or if end-of-speech is detected for all utterances (lines 19–22 of Algorithm 2). Finally, the output sequence is obtained with the most reliable hypothesis in $\hat{\mathbb{Y}}$ for each utterance (line 24 of Algorithm 2).

Algorithm 2 B-width batched beam search decoding

Input: input feature representation set $\mathbb{H} = \{\mathbf{h}_1, \cdots, \mathbf{h}_U\}$, beam width B
Output: output sequence set $\mathbb{Y} = \{\mathbf{y}_1, \cdots, \mathbf{y}_U\}$
1: $\mathbb{Y}^0_{[U\times B]} \leftarrow \{\{$<*eos*>$\}, \cdots, \{$<*eos*>$\}\}$
2: $\hat{\mathbb{Y}}_{[U]} \leftarrow \{\{\varnothing\}, \cdots, \{\{\varnothing\}\}$
3: Score_Fn($\cdot$, $\mathbb{H}$) $\leftarrow P^{joint}(\cdot|\mathbb{H})$
4: **for** $l \in \{1, \cdots, max_{h_i\in\mathbb{H}}|h_i|\}$ **do**
5: $\quad \mathbb{Y}^l_{[U\times B]} \leftarrow \{\{\varnothing\}, \cdots, \{\{\varnothing\}\}$
6: $\quad \mathbb{P}_{[U\times B,|C|]} \leftarrow$ Score_Fn($\mathbb{Y}^{l-1}$)
7: $\quad \hat{\mathbb{P}}_{[U\times B]} \leftarrow \mathbb{P}(\cdot,$ <*eos*>$)$
8: $\quad \mathbb{P}_{[U\times B,|C|]}(\cdot,$ <*eos*>$) \leftarrow$ log0
9: $\quad \mathbb{I}_{[U,B]} \leftarrow$ TopB($\mathbb{P}_{[U\times B,|C|]}$)
10: $\quad \mathbb{Y}^l_{[U\times B]} \leftarrow$ GatherB($\mathbb{Y}^{l-1}_{[U\times B]}, C, \mathbb{I}_{[U,B]}$)
11: $\quad$ **best_score** = $\left\{max_{j\in|C|}\mathbb{P}(i,j)\,|1 \le i \le U\right\}$
12: $\quad$ **for** $i \in \{1\cdots U\}$ and $j \in \{1\cdots B\}$ **do**
13: $\quad\quad p = \hat{\mathbb{P}}(i \times U + j)$
14: $\quad\quad y = \mathbb{Y}^{l-1}(i \times U + j) \circ$ <*eos*>
15: $\quad\quad$ **if** $p >$ **best_score**(i) **then**
16: $\quad\quad\quad \hat{\mathbb{Y}}(i)$ .add((y, p))
17: $\quad\quad$ **end if**
18: $\quad$ **end for**
19: $\quad$ is_eos = $\left\{\text{ENDDETECT}(\hat{\mathbb{Y}}(i), l)|1 \le i \le U\right\}$
20: $\quad$ **if** not (false $\in$ is_eos) **then**
21: $\quad\quad$ **break**
22: $\quad$ **end if**
23: **end for**
24: **return** $\left\{\text{argmax}_{(y,p)\in\hat{\mathbb{Y}}(i)}\, p|1 \le i \le U\right\}$

When compared to et al [2019d], Seki et al. [2018], this work uses the different scoring function for a CTC/Transformer-based speech recognition (line 3 of Algorithm 2) and improves an end-of-speech detection based on CTC (line 19 of Algorithm 2). For a fast decoding, this work also proposes a time-restricted CTC scoring of the scoring function.

3.2 CTC-based end-of-speech detection and time-restricted CTC prefix scoring

This section first explains a baseline end-of-speech detection et al [2017b] and then proposes fast decoding methods based on a CTC prefix score.

3.2.1 Baseline end-of-speech detection

As mentioned in Section 3.1, the beam search decoding finishes when a confident <*eos*>-ended hypothesis is detected for a fast completion. Based on et al [2017b], the baseline end-of-speech detection detects end-of-speech if the following equation is satisfied,

$$\sum_{m=0}^{M-1}\left[\left\{\max_{y\in\hat{\mathbb{Y}}(i):|y|=l-m} P(y|\mathbf{h}_i) - \max_{y'\in\hat{\mathbb{Y}}(i)} P(y'|\mathbf{h}_i)\right\} < D_{end}\right] = M. \tag{8}$$

In this work, the predefined parameters M and D_{end} are set to 3 and e^{-10}, as in et al [2017b].

Algorithm 3 Proposed CTC-based end-of-speech detection

Input: output sequence candidate set $\hat{\mathbb{Y}}(i)$, maximum length len_h
Output: whether end-of-speech is detected

```
if Eq. 8 is satisfied then
    return true
end if
count_long_hyp = 0
for y_{i,j}^{1:l} ∈ Ŷ(i) do
    if τ_{i,j}^l = len_h then
        count_long_hyp ++
    end if
    if count_long_hyp > C then
        return true
    end if
end for
return false
```

3.2.2 Proposed CTC-based end-of-speech detection

The baseline end-of-speech detection of et al [2017b] performs well in a normal condition. However, the absolute probability values of hypotheses are unreliable in a mismatched condition between training and decoding, which can occur in real-world applications. To prevent such a malfunction that slows down speech recognition, we propose a CTC-based end-of-speech detection method that uses the estimated time of the last label (<*eos*>) of each completed hypothesis.

Based on a CTC prefix score, for the j-th l-length hypothesis, $\mathbf{y}_{i,j}^{1:l}$, of an i-th feature representation, the start time index $\tau_{i,j}^{l}$ and end time index $\tilde{\tau}_{i,j}^{l}$ of the last label, $\mathbf{y}_{i,j}^{l:l}$, are estimated as follows:

$$\tau_{i,j}^{l} = \underset{\tau_{i,j}^{l-1} \leq t \leq len_h}{\operatorname{argmax}} \phi_t(\mathbf{y}_{i,j}^{1:l}) \tag{9}$$

$$\tilde{\tau}_{i,j}^{l} = \underset{\tau_{i,j}^{l-1} \leq t \leq len_h}{\operatorname{argmax}} \phi_t(\tilde{\mathbf{y}}_{i,j}^{1:l}) \tag{10}$$

where $\tilde{\mathbf{y}}$ is a text sequence that ends with a blank symbol concatenated after $\mathbf{y}$. That is, $\tau_{i,j}^{l}$ is a time index that maximizes the CTC forward probability for $\mathbf{y}_{i}^{1:l}$ within a specified time index range. Similarly, $\tilde{\tau}_{i,j}^{l}$ is one for $\tilde{\mathbf{y}}$. As shown in Fig. 2(**a**), we validate the estimated time index by obtaining the start time of the decoded output text for a Korean utterance using the proposed start time index. Note that the upper and lower parts show the waveform in yellow and its spectrum in gray for the utterance. The estimated start time is shown in red. It can be seen that the start time is nearly estimated at the start position of each syllable. On the other hand, Fig. 2(**b**) shows an example of the start time indices for a wrong hypothesis having repeatition errors, which errors can be occurred in an attention-based speech recognition. As shown in the figure, the repeatition errors are $\left\{y^{9}, \cdots, y^{12}\right\}$ and the start time indices for the errors are same as len_h=100 due to the limited search range of τ.

Based on the property that is depicted in Fig. 2(**b**), the CTC-based end-of-speech detection method is proposed, as in Algorithm 3. If the baseline end-of-speech detection method fails to predict end-of-speech, the start time index is examined for each hypothesis in the confident <*eos*>-ended hypothesis set $\hat{\mathbb{Y}}(i)$ for $\mathbf{h}_i$. If the start time index is equal to len_h more than C times, end-of-speech is detected. In this study, the parameter C was set to 2.

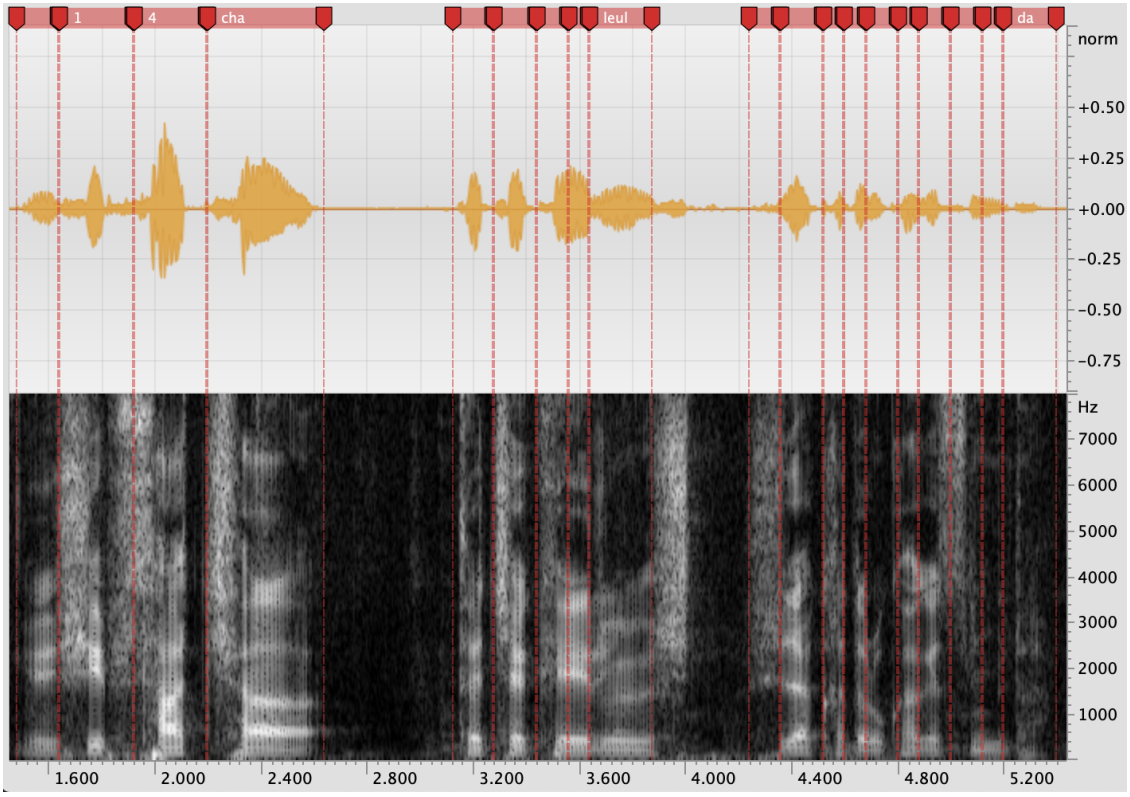
3.2.3 Proposed time-restricted CTC prefix score for fast decoding

Since the sequential calculation of a CTC prefix score limits parallel processing, we propose a CPU-based and time-restricted CTC prefix score for a joint CTC/Attention based Transformer to improve computational efficiency. The calculation of the CTC prefix score of Eq. (7) is restricted within the proposed time range, as in et al [2019d]. The proposed time-restricted CTC prefix score is defined as follows:

$$\sum_{s_{i,j}^{l} \leq t \leq e_{i,j}^{l}} \phi_{t-1}(\mathbf{y}_{i,j}^{1:l-1}|\mathbf{h}_i) p^{c}(z_t = \mathbf{y}_{i,j}^{l:l}|\mathbf{y}_{i,j}^{1:l-1}, \mathbf{h}_i), \tag{11}$$

Figure 2: Example of time information for each decoded output unit using estimated start time index.

(**a**) Illustration of the start time indices



(**b**) Start time indices for a wrong hypothesis having repeatition errors. len_h is 100 in this example.

	y^1	y^2	y^3	y^4	y^5	y^6	y^7	y^8	y^9	y^{10}	y^{11}	y^{12}
token	sil	i	1	4	cha	sil	dae	chaeg	cha	sil	dae	chaeg
Range for τ	[0,100]	[2,100]	[37,100]	[41,100]	[48,100]	[55,100]	[66,100]	[78,100]	[82,100]	[100,100]	[100,100]	[100,100]
start time τ	2	37	41	48	55	66	78	82	100	100	100	100

where $s^l_{i,j}$ and $e^l_{i,j}$ indicate the start and end times to be calculated, respectively. These are calculated as

$$s^l_{i,j} = \max(\tau^{l-1}_{i,j} - \mathrm{M}_1,\, l,\, 1), \tag{12}$$

$$e^l_{i,j} = \min(\tilde{\tau}^{l-1}_{i,j} + \mathrm{M}_2,\, |h_i|), \tag{13}$$

where M_1 and M_2 are tunable margin parameters. For the batch processing of $\mathbb{Y}^l$, the restricted range is defined as

$$s^l = \min_{1 \le i \le U,\, 1 \le j \le B} s^l_{i,j}, \tag{14}$$

$$e^l = \max_{1 \le i \le U,\, 1 \le j \le B} e^l_{i,j}, \tag{15}$$

The time-restricted CTC prefix score can be computed in a small amount of the calculation. For a small but frequent calculation in a GPU device, memory transfer load between CPU and GPU can be a bottleneck Oh et al. [2020]. Therefore, the calculation of the CTC prefix score is moved from the GPU device to a CPU device to reduce the GPU memory transfer load.

The proposed time-restricted CTC prefix score reduces the amount of computation based on the proposed estimated time information since a Transformer decoder hardly captures time information. In contrast, et al [2019d] restricted the CTC prefix score using time information from a RNN-based attention-decoder. et al [2020r] only limited the end time based on a differently estimated end time.

3.3 Offline recognition of long utterances

When it comes to the recognition of long utterances, the performance of Transformer-based end-to-end speech recognition tends to degrade significantly owing to the characteristics of the self-attention of the Transformer and the sensitivity to the utterance length of training data et al [2019e]. On the other hand, the computational complexity for a self-attention quadratically increases in proportion to the utterance length et al [2017a], Kitaev et al. [2020]. To tackle these issues, we perform segmentation before recognition. Two segmentation methods are tested. The first is a split at a short pause with a VAD, and the second is simple hard segmentation.

In et al [2020s], VAD information is used as a triggering sign for the decoder in real time. In this work, explicit segmentation is performed beforehand using a DNN-based VAD.

In conventional DNN-HMM ASR systems coupled with the language models, the recognition results are searched by back-tracking the optimal path using the Viterbi algorithm. Usually the back-tracking point is determined as an end of utterance. However, for long speeches, finding the relevant short pauses and using them as back-tracking points makes it possible to generate ASR results quickly and hence to reduce the user perceived latency.

Finding short pauses or detecting voice activity in continuous speech is a difficult task and one of the oldest topics in speech-related researches. Traditionally the methods to track the energies of speech and non-speech are commonly used. These methods suffer when signal-to-noise ratio(SNR) is dynamically changes. In authors' previous work, outputs of acoustic model (AM) have been successfully utilized to detect voice activity in DNN-HMM based ASR systems.

In DNN-HMM based ASR systems, a deep neural network is trained so that each output node estimates a posteriori probability of a state given an input feature vector $\mathbf{x_t}$ at time t, $P(s_k|\mathbf{x_t})$, where a state s_k corresponds to the part of a phoneme. The probabilities are directly used as the AM scores which are combined with language model scores to find optimal ASR results.

In previous work, these probabilities are successfully used to compute probabilities of voice presence in input signal as following.

Let o_i^t be the output value of the i-th node of the neural network at time t. Then, speech presence probability ($P_{\mathcal{S}}(t)$) and speech absence probability ($P_{\mathcal{N}}$) at time t are estimated as

$$\log P_{\mathcal{S}}(t) \approx \max_{k \in \mathcal{S}} o_k^t \tag{16}$$

$$\log P_{\mathcal{N}}(t) \approx \max_{k \in \mathcal{N}} o_k^t \tag{17}$$

$$\mathrm{LLR}(t) = \log P_{\mathcal{N}}(t) - \log P_{\mathcal{S}}(t) \tag{18}$$

where $k \in \mathcal{S}$, and $k \in \mathcal{N}$ are output nodes corresponding to the speech and noise states, respectively. A frame is regarded as a non-speech frame if the log-likelihood ratio $\mathrm{LLR}(t)$ is larger than a given threshold. To obtain a more robust decision, the frame-wise results are smoothed over multiple frames, as in Oh et al. [2020].

We re-used DNN-based VAD algorithm to segment long speeches for Transformer-based end-to-end speech recognition system. Segmentation based on DNN-VAD produces good performance in splitting long utterances in general; however, this requires significant computation resources. In DNN-HMM based ASR systems, these probabilities are computed for ASR and there are no extra computation for VAD. But for the Transformer-based end-to-end speech recognition system, there is no such component like AM and this computation is only for the VAD, which requires heavy computation with GPU for large DNN models.

It is also possible to use the simpler VAD algorithm as in Park [2013]. In this work, we attempted hard segmentation by segment length, i.e., splitting long utterances into short pieces of the same length while not considering truncation. Hard segmentation requires no computation, and the resulting segments are of the same length. This reinforces the merits of the batch processing in Section 3.1.

4 Experiments

4.1 Baseline ASR system and speech corpus

4.1.1 Transformer-based end-to-end model

The Transformer model of the end-to-end speech recognizer used in this study was trained using ESPnet, an end-to-end speech processing toolkit et al [2018b], and the decoding was performed using the modified version of the toolkit. During the decoding, an attention cache was applied in all experiments for speedup et al [2019f].

As an input feature, 80-dimensional log-Mel filterbank coefficients were extracted for every 10–ms analysis frame. The pitch feature was not used because in the Korean language, tone and pitch are not important features. During training and decoding, a global cepstral mean and variance normalization was applied to the feature vectors.

Most hyperparameters for the Transformer model, inherit values from the default settings of the toolkit. The encoder consists of two convolutional layers, a linear projection layer, and a positional encoding layer followed by 12 self-attention blocks with layer-normalization. An additional linear layer was utilized for CTC. The decoder has six self-attention and encoder-decoder attention blocks. For every Transformer layer, we used 2048-dimensional feedforward networks and four attention heads with 256 dimensions. The training was performed using the Noam optimizer et al [2017a], warmup steps, label smoothing, gradient clipping, and accumulating gradients et al [2018c]. 100 epochs of training were performed without early stopping.

The text tokenization was performed in terms of character units. In Korean, a character consists of two or three graphemes and corresponds to a syllable. Although the number of plausible characters in Korean is greater than 10,000, only 2,273 tokens are used as output symbols, including digits, alphabets, and a spacing symbol, which are seen in a training corpus. No other text processing was performed except for the removal of punctuation marks and tokenization.

4.1.2 Speech Corpus

To train the end-to-end ASR model, we utilized approximately 12.4k hours of Korean speech corpus, which consist of a variety of sources including read digits and sentences, recordings of spontaneous conversation, and mostly (about 11.1k hours) broadcast data et al [2020t]. Therefore, the training data contain various utterance lengths. All sentences were manually transcribed, and long sentences were automatically segmented using the transcription and aligning process. Utterances longer than 30 s were excluded when training.

As for the test corpus, meetings at a public office were recorded. An automatic meeting transcription system was introduced for evaluation purposes. In total, 8 h of recording were made from seven meetings. In each meeting, 4–22 people participated, and every participant had his or her own gooseneck-type microphone. Each microphone was turned on only while the corresponding speaker uttered, and this was recorded separately. However, there were some overlaps and crosstalk from adjacent speakers, which were ignored in the manual transcription. Each recording lasted from 5 s to 36 min and was manually transcribed and split according to the content by human transcribers. Each segment was of 0.6–42.9 s. The number and average lengths of segments are shown in the first row of Table 5.

We performed ASR experiments to verify our proposed methods using two corpora: the Librispeech corpus, a well-known English corpus; and a real-world test dataset and the large training corpus explained in Section 4.1.2.

For experiments with the Librispeech corpus, one of the best models published by ESPnet group was downloaded and used for decoding [2]. The speech recognition performance in word error rate (WER) and the recognition speed are measured as a real-time factor (xRT), which is the elapsed time divided by the utterance length, to recognize a total 10.7 h of test speeches.

For the Korean test set, we trained a Transformer as described in Section 4.1. The accuracy was measured as character error rates (CER) instead of the word error rate (WER) because of ambiguity in the word spacing. The recognition speed was measured as an xRT to recognize 8 h of the test set. For both sets, the xRTs were averaged after three trials.

All experiments in this section were performed on a workstation with two Xeon Gold 5122 CPUs and two GPU cards of a GeForce RTX 2080 Ti, which has 11.0 GB of GPU memory.

4.2 Experiments for batch decoding

First, experiments to verify the effect of batch decoding are performed. As a baseline, we used the Transformer-based end-to-end ASR of Section 4.1.1 and performed a single-utterance multiple-hypothesis B-width beam search decoding on two GPUs. At each decoding step, the $B(= 3)$ hypotheses were batched, and the probabilities were computed in parallel. Multiple-utterance multiple-hypothesis batched decoding considers different lengths of multiple utterances. However, the baseline ASR does not because it performs one utterance at a time.

Experimental results with Librispeech are listed in Table 1. Batchsize is set to 16 to fit in the GPU memory. As shown in the table, multiple-utterance multiple-hypothesis batch decoding could recognize utterances 5.9 times faster with the same accuracy. As for two cases of the baseline and the baseline without language model(LM) with narrow beam, the xRTs are not presented because it was impractical to measure them. It took more than a few hours to decode 10.7 hours of test data, since the baseline system is not optimized for the fast decoding at all.

[2] A Transformer model was retrieved from `espnet/egs/librispeech/asr1/RESULTS.md`

Table 1: Performance of baseline Transformer-based ASR employing 3-width single-utterance multiple-hypothesis beam search, and proposed ASR employing 3-width multiple-utterance multiple-hypothesis beam search on Librispeech evaluation set and model trained on 960-h trainset. Experiments are performed using two GPUs. Total utterance duration is 10.7 h.

Configuration	test_ clean	test_ other	xRT
Baseline	3.29	6.89	-
No LM and narrow beam(=3.0)	3.94	8.63	-
Ours, batchsize=1	3.92	8.77	4.75e-2
Ours, batchsize=16	3.93	8.75	7.99e-3

Table 2: Performance of baseline ASR and proposed algorithm employing multiple-utterance batched beam search, CTC-based end-of-speech detection, and restricted CTC prefix score. Real-world Korean speech data are used.

Method	CER(%)	xRT
baseline	9.06	2.56e-1
+ batched decoding	9.03	1.88e-2
+ CPU CTC decoding	9.06	1.15e-2
+ CTC end-of-speech detection	9.08	1.05e-2
+ restricted CTC, M_1=5,M_2=∞	9.07	9.11e-3
+ restricted CTC, M_1=5,M_2=60	9.08	7.31e-3
+ restricted CTC, M_1=5,M_2=40	9.10	7.28e-3
+ restricted CTC, M_1=5,M_2=20	9.14	6.93e-3

The accuracy of baseline with no LM and narrow beam should be same as that of ours when batchsize is one, but it is slightly different; for test-clean 3.94 vs 3.92, and for test-other 8.63 vs 8.77. This is because the feature extraction module is slightly different partly because of implementation issues and also because of the dithering process in feature extraction. Dithering is used to prevent zeros in the filterbank energy computation by adding random noises to input signal.

The accuracy fluctuation depending on the batchsize (third and forth rows in Table 1 is induced from the zero padding whiling making a batch. To make a batch of multiple utterances, the zeros are padded to shorter inputs to make the same length for the all utterances in the same batch. Padded zeros are masked by end-of-sentence(eos) detection algorithm, but still the zeros at eos boundaries affects the computation and hence results in slightly different ASR results.

As for the Korean real-world test set, the baseline ASR achieves a CER of 9.06% and average xRT of 0.256, as shown in Table 2. As a comparison, our previously developed conventional DNN-HMM based ASR system using five-layer bidirectional long short-term model (bi-LSTM) trained with the same training corpus achieved a CER of 14.72% with an external LM.

To speed up the recognition by utilizing batch processing, the order of segments is sorted by their lengths to process utterances of similar lengths in the same batch. For fast speech recognition, we gradually performed the batched beam search in Section 3.1 using a batch size of 21, moved the CTC prefix score calculation to the CPU, and performed the end-of-speech detection of Section 3.2. As shown in the second, third, and forth rows of Table 2, the decoding time is reduced to 543 s, 331 s, and 303 s with considerable accuracy. The decoding time reduction is obtained owing to accelerating parallelization, the prevention of sequential processing, and quickly detecting end-of speech. To investigate the effect of the proposed end-of-speech detection method, we calculate the cumulative histogram of the time index of the end-of-speech using the baseline method and the proposed method, respectively, as shown in Fig. 3. Note that the values on the x-axis are time-index bins of detected end-of-speech; and the values on the y-axis are the normalized accumulated occurrence for each bin. From the figures, we observe that the proposed method quickly detects end-of-speech without loss of the recognition accuracy compared to the baseline method.

For a further speedup, the restricted CTC prefix score of Section 3.2 can be applied. First, we restricted the start time of the CTC prefix score with M_1 of 5 and then an end time with M_2 of 60, 40, or 20. From the fifth row of Table 2, the decoding time was reduced to 263 s with comparable accuracy if only the start time is restricted. From the last three rows of Table 2, the decoding time is further reduced to 211 s, 210 s, and 200 s, with an accuracy degradation according to M_2 when the end time is restricted.

Table 3: Dependency of word error rate and recognition speed on length of input utterance.

Utterance Len(sec)	Avg. Len(sec)	test-clean		test-other		Speed
		# Utts	WER	# Utts	WER	In xRT
0–5	3.4	1097	4.45	1422	10.09	0.024
5–10	7.1	913	3.25	1029	8.21	0.032
10–15	12.2	373	2.96	318	7.20	0.045
15–20	17.1	148	3.19	124	7.27	0.053
20–	24.1	89	8.79	46	12.25	0.069
all	-	2620	3.97	2939	8.60	0.040

Table 4: Dependency of word error rate and recognition speed on length of input utterance for the concatenated test data. Original utterances are concatenated to constitute longer sentences with maximum lengths of 10, 20, 30, 40, and 50 seconds respectively.

Utterance Len(sec)	Avg. Len(sec)	test-clean		test-other		Speed
		# Utts	WER	# Utts	WER	In xRT
–10	9.2	2034	3.83	2163	8.48	0.041
–20	16.0	1218	3.87	1192	8.37	0.054
–30	23.9	786	12.60	763	18.29	0.075
–40	34.8	566	30.98	545	37.05	0.101
–50	44.6	438	46.52	428	52.52	0.135

4.3 Decoding time versus utterance length

One of the most significant drawbacks of the Transformer model is its weakness in long sequences because self-attention in each layer computes the output using the relationship between entire input sequences. It is well-known that the computation complexity is proportional to the square of the input length et al [2017a], Kitaev et al. [2020].

In this section, the effect of the sequence length is analyzed using the Librispeech dataset and the model used in the previous section. The utterances in the Librispeech dataset are short in length, and the longest utterance is 35 s long. All utterances in the test set are grouped by lengths as 0–5, 5–10, 10–15, 15–20, and longer than 20 s, and they are decoded separately to measure the accuracy and recognition speed. The results are shown in Table 3 in two test sets: test-clean and test-other. The two sets are decoded together to measure the xRTs. The error rates are computed separately.

As shown in Table 3, the error rates are much higher for the group with the longest utterances. The accuracy is best with 10–20-s-long utterances. The recognition speed in xRT increases as the lengths are increased.

To see the effect of the utterance lengths on the recognition performance more closely, the utterances in the Librispeech test set are concatenated to produce longer sentences and then fed into the decoder. The reference transcriptions are also concatenated accordingly. The concatenation is accomplished as follows: for a given predefined maximum length L and an ordered list of test data, the utterances from the top of the list are concatenated not to exceed length L. If the next utterance makes the concatenated sentence longer than L, then the utterance becomes the beginning of the new sentence, and the next utterances are concatenated onto this sentence.

As for the maximum length of $L = 10,\ 20,\ 30,\ 40$ and 50, the test sets are generated, and then WER and xRT are measured in the same way as in Table 3. The results are presented in Table. 4 and also shown in Fig. 4. Note that the values on the x-axis are the average length of concatenated sentences and are shorter than the maximum lengths. It is clear that the longer the sentences, the higher the error rates, and the longer it takes to be decoded.

In many real-world speech recognition applications, users speak continuously and spontaneously as in video captioning. Hence it is important to recognize long utterances quickly and accurately. In a next section, a method to efficiently decode long utterances is explained.

4.4 Recognition of long utterance by segmentation

As presented in the previous section, the input length has great influence on the performance of the Transformer model. In Section 4.2, to recognize speech with a Transformer model, manually segmented utterances are used. However, manual segmentation cannot be accomplished for large test corpus in real-world applications. To overcome this issue, we present two automatic segmentation methods in this section.

Table 5: Statistics of length and number of segments before and after splitting.

Method	Num. of segments	Avg. Length	Std. Dev
Source	83	347.7	464.4
Manual	1,173	22.8	7.28
DNN-VAD	1,838	15.7	2.79
Hard Seg.	1,445	20.0	1.34

Table 6: Recognition accuracy in CER (%) and averaged xRT after three trials. Allowed batch size is largest applicable in experiment.

Method	CER	xRT	Allowed batchsize
Manual	9.10	6.98e-3	21
DNN-VAD	10.73	5.83e-3	66
Hard Seg.	12.22	6.39e-3	64

First, we applied DNN-based VAD, which split 83 utterances into 8620 short pieces. These had an average length of 3.34 s and maximum length of 12 s. Consecutive short pieces are merged into a segment of longer than minimum length, and pieces longer than the maximum length are split again uniformly. Second, hard segmentation is applied so that the lengths of resulting segments are between minimum and maximum length and are as uniform as possible, including the last segment. The lengths and numbers of segments for the two methods are given in Table 5. For DNN-VAD, min and max lengths are set to 15 and 20 s, respectively; and for hard segmentation they are set to 19 and 20 s. These values are selected in consideration of the batch size allowed for the GPU cards used in the experiments. The segmented utterances are fed into the end-to-end recognizer corresponding to the seventh row of Table 2. Table 6 shows the recognition performance and speed. The accuracy with hard segmentation is worse than the DNN-VAD segmentation as well as the manual segmentation, since it splits an utterance at any points randomly even in the middle of a word and words at boundary are recognized incorrectly. DNN-VAD segmentation method splits utterances in short pauses, which are usually boundaries of phrases.

The difference in CERs between manual segmentation and DNN-VAD is mainly owing to insertion errors since in manual segmentation, overlapped speeches that are difficult to transcribe are trimmed. The accuracy drop in hard segmentation is owing to the deletions at segmented boundaries. Further work is ongoing to reduce this type of error.

Also the number of segments with DNN-VAD is larger than the manual and the hard segmentation and the lengths of segments are shorter as shown in Table 5. Thus we could use larger batchsize with DNN-VAD segmentation and the recognition is faster than with other segmentation methods. However as pointed out in Section 3.3, DNN-VAD requires extra computation with GPUs to compute DNN outputs, which prevents the method to be used in commercial use to decode massive data and the hard segmentation method is preferred over the DNN-VAD.

5 Conclusion

The Transformer model is being actively used in many research areas yielding a state-of-the-art performance, and in the field of ASR, the model is leading the scoreboard. In this work, various methods to bring the model into practical use were proposed and verified.

This paper proposed fast and efficient recognition methods to utilize offline Transformer-based end-to-end speech recognition in real-world applications equipped with low computational resources. For fast decoding, we adopted a multiple-utterance multiple-hypothesis batched beam search for a Transformer-based ASR to accelerate a GPU parallelization. The proposed CTC-based end-of-speech detection could quickly complete the searching process, thus speeding up the recognition. This is more effective for noisy and sparsely uttered utterances, where mismatches between training and testing conditions are significant. Moreover, the proposed CPU-based and time-restricted CTC prefix score reduced the computational complexity by limiting the time range to be examined for each decoding step. For the efficient decoding of long speeches, we proposed to split long speeches into segments using two methods: (a) DNN-VAD-based segmentation and (b) hard segmentation. The DNN-VAD based segmentation achieved better recognition accuracy than the hard segmentation. However, the DNN-VAD based segmentation required a significant amount of computation resources, while hard segmentation could be done without additional computation. The segmentation of long speeches makes possible stable recognition of speech from various applications with Transformer models using limited GPU memories. This ensures stable accuracy and fast speed by boosting the proposed batch processing.

Speech recognition experiments were performed on the Librispeech dataset to verify the proposed algorithm. Experiments were performed on a real-world Korean speech dataset recorded at meetings with multiple speakers. For the 8 h of speech after being segmented, speech-to-text conversion was undertaken for less than 3 min by a Transformer-based end-to-end ASR system employing the proposed method with two GPU cards. Moreover, the ASR system achieved a CER of 10.73%, which is 27.1% lower than that of the conventional DNN-HMM based ASR system.

6 Acknowledgement

This work was supported by Institute for Information & communications Technology Planning & Evaluation(IITP) grant funded by the Korea government(MSIT) (No.2019-0-01376, Development of the multi-speaker conversational speech recognition technology)

References

A. B. Nassif et al. Speech recognition using deep neural networks: a systematic review. *IEEE Access*, 7:19143–19165, 2019a.

V. Roger, J. Farinas, and J. Pinquier. Deep neural networks for automatic speech processing: a survey from large corpora to limited data. In *arXiv preprint, CoRR*, 2020.

J. Li et al. On the comparison of popular end-to-end models for large scale speech recognition. In *in Proc. Conf. Int. Speech Commun. Assoc.*, pages 1–5, Shanghai, China, Dec. 2020a.

H. Chung, J. G. Park, and H. Jung. Rank-weighted reconstruction feature for a robust deep neural network-based acoustic model. *ETRI J.*, 41(2):235–241, 2019.

I. Sutskever, O. Vinyals, and O. V. Le. Sequence to sequence learning with neural networks. In *in Proc. Adv. Neural Info. Proc. Sys.*, volume 27, Montreal, Canada, Dec. 2014.

D. Bahdanau, K. Cho, and Y. Bengio. Neural machine translation by jointly learning to align and translate. In *in Proc. Int. Conf. Learn. Represent.*, San Diego, CA, USA, May 2015.

A. Vaswani et al. Attention is all you need. In *in Proc. Adv. Neural Info. Proc. Sys.*, volume 30, Long Beach, CA, USA, Dec. 2017a.

L. Dong, S. Xu, and B. Xu. Speech-Transformer: a no-recurrence sequence-to-sequence model for speech recognition. In *in Proc. IEEE Int. Conf. Acoust., Speech Signal Process.*, pages 5884–5888, Calgary, Canada, Apr. 2018.

N. Moritz, T. Hori, and J. L. Roux. Streaming end-to-end speech recognition with joint CTC-attention based models. In *in Proc. IEEE Workshop Auto. Speech Recog. Understanding*, pages 936–943, Sentosa, Singapore, Dec. 2019.

N. Moritz, T. Hori, and J. Le. Streaming automatic speech recognition with the Transformer model. In *in Proc. IEEE Int. Conf. Acoust., Speech Signal Process.*, pages 6074–6078, Barcelona, Spain, Mar. 2020.

H. Hwang and C. Lee. Linear-time Korean morphological analysis using an action-based local monotonic attention mechanism. *ETRI J.*, 42(1):101–107, 2020.

S. H. K. Parthasarathi and N. Strom. Lessons from building acoustic models with a million hours of speech. In *in Proc. IEEE Int. Conf. Acoust., Speech Signal Process.*, pages 6670–6674, Brighton, UK, May 2019.

S. Zhou, S. Xu, and B. Xu. Multilingual end-to-end speech recognition with a single Transformer on low-resource languages. In *arXiv preprint, CoRR*, 2018.

S. Zhou et al. Syllable-based sequence-to-sequence speech recognition with the Transformer in Mandarin Chinese. In *in Proc. Conf. Int. Speech Commun. Assoc.*, pages 791–795, Hyderabad, India, Sep. 2018a.

S. Karita et al. A comparative study on Transformer vs RNN in speech applications. In *in Proc. IEEE Workshop Auto. Speech Recog. Understanding*, pages 449–456, Sentosa, Singapore, Dec. 2019b.

A. Gulati et al. Conformer: convolution-augmented Transformer for speech recognition. In *in Proc. Conf. Int. Speech Commun. Assoc.*, pages 5036–5040, Shanghai, China, Dec. 2020b.

W. Huang et al. Conv-Transformer Transducer: low latency, low frame rate, streamable end-to-end speech recognition. In *in Proc. Conf. Int. Speech Commun. Assoc.*, pages 5001–5005, Shanghai, China, Dec. 2020c.

S. Karita et al. Improving Transformer-based end-to-end speech recognition with connectionist temporal classification and language model integration. In *in Proc. Conf. Int. Speech Commun. Assoc.*, pages 1408–1412, Graz, Austria, Sep. 2019c.

H. Miao et al. Transformer-based online CTC/attention end-to-end speech recognition architecture. In *in Proc. IEEE Int. Conf. Acoust., Speech Signal Process.*, pages 6084–6088, Barcelona, Spain, Mar. 2020d.

X. Chang et al. End-to-end multi-speaker speech recognition with Transformer. In *in Proc. IEEE Int. Conf. Acoust., Speech Signal Process.*, pages 6134–6138, Barcelona, Spain, Mar. 2020e.

Y. Higuchi et al. Mask CTC: non-autoregressive end-to-end ASR with CTC and mask predict. In *in Proc. Conf. Int. Speech Commun. Assoc.*, pages 3655–3659, Shanghai, China, Dec. 2020f.

Y. Fujita et al. Insertion-based modeling for end-to-end automatic speech recognition. In *in Proc. Conf. Int. Speech Commun. Assoc.*, pages 3660–3664, Shanghai, China, Dec. 2020g.

T. Parcollet, M. Morchid, and G. Linarès. E2E-SINCNET: toward fully end-to-end speech recognition. In *in Proc. IEEE Int. Conf. Acoust., Speech Signal Process.*, pages 7714–7718, Barcelona, Spain, Mar. 2020.

X. Zhou et al. Self-and-mixed attention decoder with deep acoustic structure for Transformer-based LVCSR. In *in Proc. Conf. Int. Speech Commun. Assoc.*, pages 5016–5020, Shanghai, China, Dec. 2020h.

Y. Higuchi et al. Improved mask-CTC for non-autoregressive end-to-end ASR. In *arXiv preprint, CoRR*, 2020i.

T. Moriya et al. Self-distillation for improving CTC-Transformer-based ASR systems. In *in Proc. Conf. Int. Speech Commun. Assoc.*, pages 546–550, Shanghai, China, Dec. 2020j.

T. Hori et al. Transformer-based long-context end-to-end speech recognition. In *in Proc. Conf. Int. Speech Commun. Assoc.*, pages 5011–5015, Shanghai, China, Dec. 2020k.

Y. Zhao et al. Cross attention with monotonic alignment for speech Transformer. In *in Proc. Conf. Int. Speech Commun. Assoc.*, pages 5031–5035, Shanghai, China, Dec. 2020l.

Y. Lu et al. Bi-encoder Transformer network for Mandarin-English code-switching speech recognition using mixture of experts. In *in Proc. Conf. Int. Speech Commun. Assoc.*, pages 4766–4770, Shanghai, China, Dec. 2020m.

G. I. Winata et al. Adapt-and-adjust: overcoming the long-tail problem of multilingual speech recognition. In *arXiv preprint, CoRR*, 2020n.

L. Kürzinger et al. Lightweight end-to-end speech recognition from raw audio data using Sinc-convolutions. In *in Proc. Conf. Int. Speech Commun. Assoc.*, pages 1659–1663, Shanghai, China, Dec. 2020o.

S. Li et al. Improving Transformer-based speech recognition with unsupervised pre-training and multi-task semantic knowledge learning. In *in Proc. Conf. Int. Speech Commun. Assoc.*, pages 5006–5010, Shanghai, China, Dec. 2020p.

D. Amodei et al. Deep Speech 2 : end-to-end speech recognition in English and Mandarin. In *in Proc. Int. Conf. Machine Learning*, pages 173–182, New York, NY, USA, June 2016.

H. Braun et al. GPU-accelerated Viterbi exact lattice decoder for batched online and offline speech recognition. In *in Proc. IEEE Int. Conf. Acoust., Speech Signal Process.*, pages 7874–7878, Barcelona, Spain, Mar. 2020q.

Y. R. Oh, K. Park, and J.G. Park. Online speech recognition using multichannel parallel acoustic score computation and deep neural network (DNN)-based voice-activity detector. *Appl. Sci.*, 10(12), 2020.

H. Seki, T. Hori, and S. Watanabe. Vectorization of hypotheses and speech for faster beam search in encoder decoder-based speech recognition. In *arXiv preprint, CoRR*, 2018. URL `arXiv:cs/1811.04568`.

H. Seki et al. Vectorized beam search for CTC-attention-based speech recognition. In *in Proc. Conf. Int. Speech Commun. Assoc.*, pages 3825–3829, Graz, Austria, Sep. 2019d.

A. Graves et al. Connectionist temporal classification: labelling unsegmented sequence data with recurrent neural networks. In *in Proc. Int. Conf. Machine Learning*, page 369–376, Pittsburgh, PA, USA, June 2006.

H. Miao et al. Online hybrid CTC/attention end-to-end automatic speech recognition architecture. *IEEE TASLP*, 28: 1452–1465, 2020r.

T. Yoshimura et al. End-to-end automatic speech recognition integrated with CTC-based voice activity detection. In *in Proc. IEEE Int. Conf. Acoust., Speech Signal Process.*, pages 6999–7003, Barcelona, Spain, Mar. 2020s.

T. Hori, S. Watanabe, and J. Hershey. Joint CTC/attention decoding for end-to-end speech recognition. In *in Proc. Ann. Mtg. Assoc. Comp. Ling.*, pages 518–529, Vancouver, Canada, July 2017.

C. Meister, T. Vieira, and R. Cotterell. Best-first beam search. *TACL*, 8:795–809, 2020.

S. Watanabe et al. Hybrid CTC/attention architecture for end-to-end speech recognition. *IEEE J-STSP*, 11(8):1240–1253, 2017b.

P. Zhou et al. Improving generalization of Transformer for speech recognition with parallel schedule sampling and relative positional embedding. In *arXiv preprint, CoRR*, volume abs/1911.00203, 2019e.

N. Kitaev, L. Kaiser, and A. Levskaya. Reformer: the efficient Transformer. In *in Proc. Int. Conf. Learn. Represent.*, Addis Ababa, Ethiopia, Apr. 2020.

K. Park. A robust endpoint detection algorithm for the speech recognition in noisy environments. In *in Proc. INTER-NOISE and NOISE-CON Congress and Conf.*, volume 247, pages 5790–5795, Innsbruck, Austria, Sep. 2013.

S. Watanabe et al. ESPnet: end-to-end speech processing toolkit. In *in Proc. Conf. Int. Speech Commun. Assoc.*, pages 2207–2211, Hyderabad, India, Sep. 2018b.

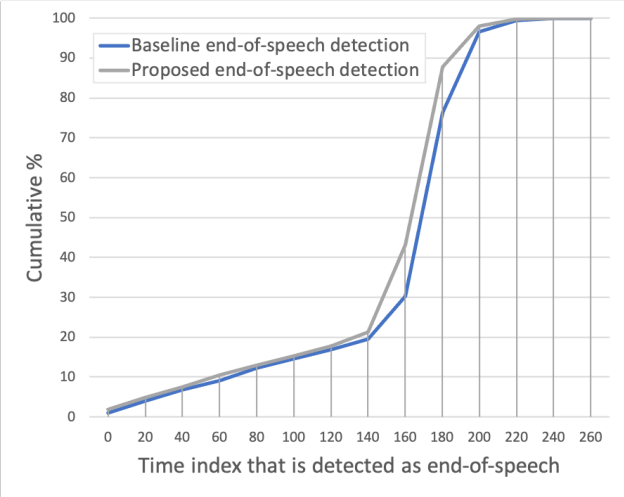
T. Xiao et al. Sharing attention weights for fast Transformer. In *in Proc. Int. Jnt. Conf. AI*, pages 5292–5298, Macao, China, Aug. 2019f.

M. Ott et al. Scaling neural machine translation. In *in Proc. Conf. Machine Translation*, pages 1–9, Brussels, Belgium, Oct. 2018c.

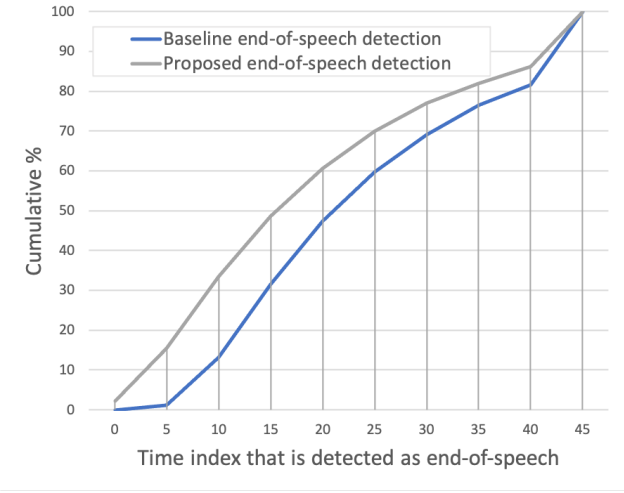
J. Bang et al. Automatic construction of a large-scale speech recognition database using multi-genre broadcast data with inaccurate subtitle timestamps. *IEICE Trans Inf Syst*, E103.D(2):406–415, 2020t.

Figure 3: Cumulative histogram of time index of end-of-speech using baseline and proposed end-of-speech detection methods, respectively.

(**a**) realworld Korean speech



(**b**) Librispeech test-clean



(**c**) Librispeech test-other

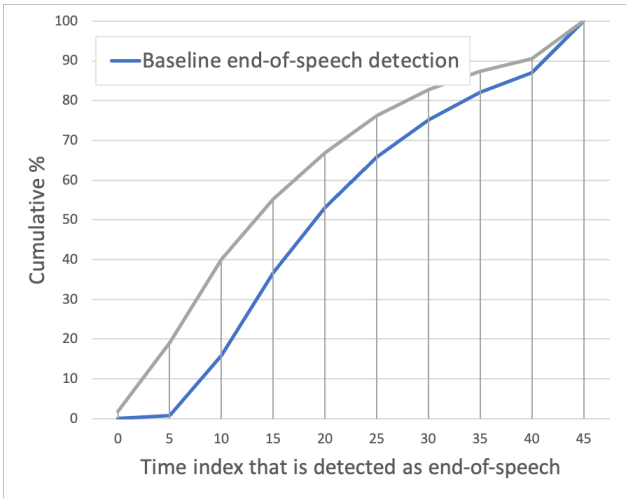
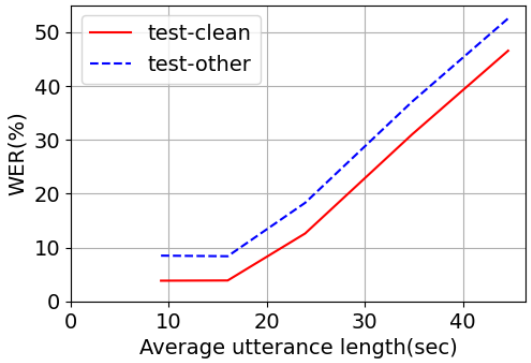


Figure 4: Dependency of word error rate and recognition speed on length of input utterance. The values in Table. 4 are shown as graphs. Note that the values on x-axis are average lengths, which are slightly less than maximum lengths.

(**a**) Average length vs. WER



(**b**) Legnth vs. xRT

